

1 Extending FreeSurfer to estimate sulcal morphology

2 Christopher R. Madan

3 School of Psychology

4 University of Nottingham

5 Nottingham, United Kingdom

6

7 Corresponding author:

8 Christopher R. Madan

9 School of Psychology, University of Nottingham

10 Nottingham, NG7 2RD, United Kingdom

11 christopher.madan@nottingham.ac.uk

12 Abstract

13 While it is well established that cortical morphology differs in relation to a variety of
14 inter-individual factors, it is often characterized using estimates of volume, thickness,
15 surface area, or gyrification. Here I developed a computational approach for estimating
16 sulcal width and depth that relies on cortical surface reconstructions output by
17 FreeSurfer. While other approaches for estimating sulcal morphology exist, studies
18 often are require the use of multiple brain morphology programs that have been
19 shown to differ in their approaches to localize sulcal landmarks, yielding
20 morphological estimates based on inconsistent boundaries. To demonstrate the
21 approach, sulcal morphology was estimated in three large sample of adults across the
22 lifespan, in relation to aging. A fourth sample is additionally used to estimate
23 test-retest reliability of the approach. This toolbox is now made freely available as
24 supplemental to this paper: <https://cmadan.github.io/calcSulc/>.

25

26 **Keywords:** sulcal width; sulcal depth; age; cortical structure; atrophy; gyrification;
27 cerebral sulci

28 Extending FreeSurfer to estimate sulcal morphology

29 **1 Introduction**

30 Cortical structure differs between individuals. It is well known that cortical thickness
31 generally decreases with age (Fjell et al., 2009; Hogstrom et al., 2013; Hutton et al., 2009;
32 Lemaitre et al., 2012; Madan & Kensinger, 2016, 2018; McKay et al., 2014; Salat et al.,
33 2004; Sowell et al., 2003, 2007); however, a more visually prominent difference is the
34 widening of sulci, sometimes described as “sulcal prominence” (Coffey et al., 1992;
35 Drayer, 1988; Jacoby et al., 1980; Laffey et al., 1984; Tomlinson et al., 1968; Yue et al.,
36 1997). In the literature, this measure has been referred to using a variety of names,
37 including sulcal width, span, dilation, and enlargement, as well as fold opening. With
38 respect to aging and brain morphology, sulcal width has been assessed qualitatively by
39 clinicians as an index of cortical atrophy (Coffey et al., 1992; Drayer, 1988; Laffey et al.,
40 1984; Pasquier et al., 1996; Scheltens et al., 1997; Tomlinson et al., 1968). An illustration
41 of age-related differences in sulcal morphology is shown in Figure 1.

42 Using quantitative approaches, sulcal width has been shown to increase with age
43 (Kochunov et al., 2005, 2008; Liu et al., 2010, 2013) likely relating to subsequent
44 findings of age-related decreases in cortical gyrification (Cao et al., 2017; Hogstrom et
45 al., 2013; Madan & Kensinger, 2016, 2018; Madan, 2018a). Sulcal widening has also
46 been shown to be associated with decreases in cognitive abilities (Liu et al., 2011) and
47 physical activity (Lamont et al., 2014). With respect to clinical conditions, increased
48 sulcal width has been found in dementia patients relative to healthy controls
49 (Andersen et al., 2015; Hamelin et al., 2015; Huckman et al., 1975; Liu et al., 2012; Ming
50 et al., 2015; Plocharski & Østergaard, 2016; Reiner et al., 2012), as well as with
51 schizophrenia patients (Largen et al., 1984; Palaniyappan et al., 2015; Rieder et al., 1979)
52 and mood disorders (Elkis et al., 1995).

53 One of the most common programs for conducting cortical surface analyses is
54 FreeSurfer (Fischl, 2012). Unfortunately, though FreeSurfer reconstructs cortical
55 surfaces, it does not estimate sulcal width or depth, leading researchers to use

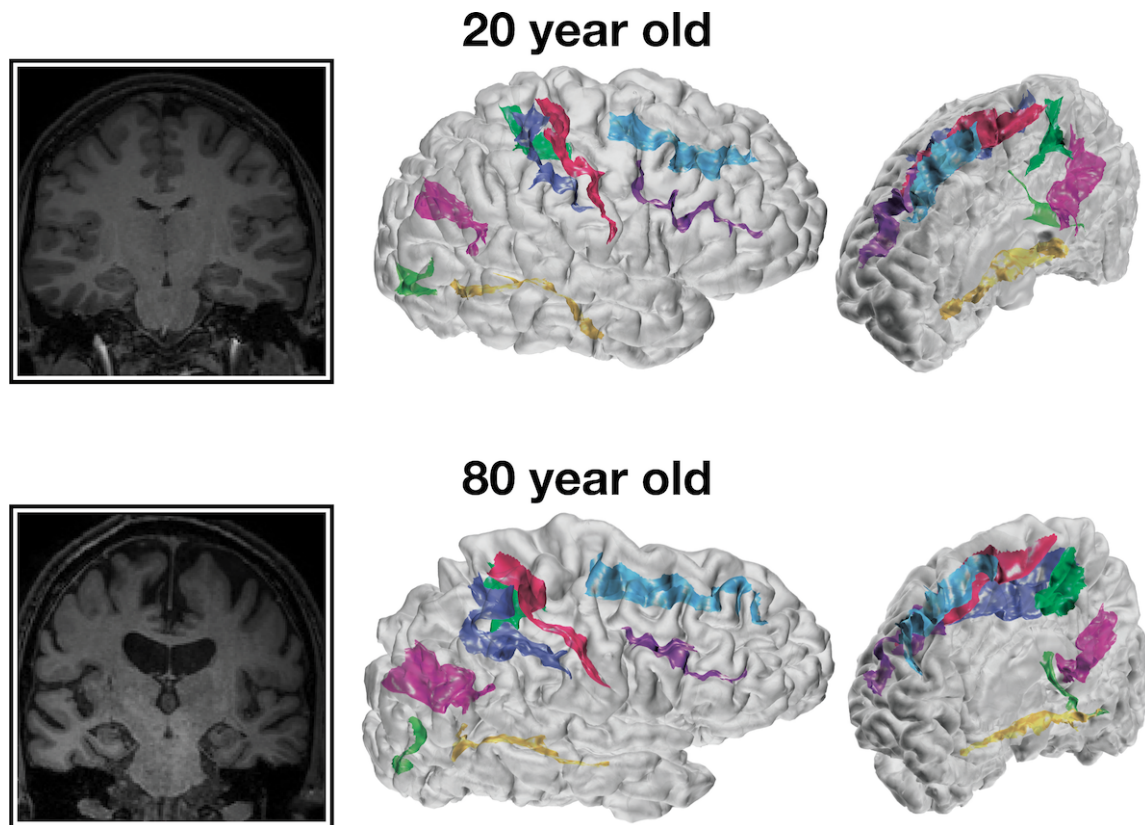


Figure 1. Representative coronal slices and cortical surfaces with sulcal identification for 20- and 80-year-old individuals.

56 FreeSurfer along with another surface analysis program, BrainVISA (Kochunov et al.,
57 2012; Mangin, Rivière, et al., 2004; Mangin, Riviere, et al., 2004; Rivière et al., 2002), to
58 characterize cortical thickness along with sulcal morphology (e.g, Cai et al., 2017;
59 Lamont et al., 2014; Liu et al., 2011, 2013; Pizzagalli et al., 2017). While this combination
60 allows for the estimation of sulcal morphology in addition to standard measures such
61 as cortical thickness, FreeSurfer and BrainVISA rely on different anatomical landmarks
62 (Mikhael et al., 2018) which can yield differences in their resulting cortical surface
63 reconstructions (Lee et al., 2006). Admittedly, determining the boundaries for
64 individual sulci and incorporating individual cortical variability is difficult (John et al.,
65 2006; Mikhael et al., 2018; Ono et al., 1990; Welker, 1990). While an ennumerate amount
66 of other methods have already been proposed to identify and characterize sulcal
67 morphology (e.g., Andreasen et al., 1994; Auzias et al., 2015; Beeston & Taylor, 2000;
68 Behnke et al., 2003; Eskildsen et al., 2005; Im et al., 2010; Jones et al., 2000; Le Goualher

69 et al., 1996, 1998; Li et al., 2008; Lohmann & von Cramon, 2000; Lohmann et al., 2008;
70 Nowinski et al., 1996; Oguz et al., 2008; Perrot et al., 2011; Royackkers et al., 1999;
71 Thompson et al., 1996; Vaillant & Davatzikos, 1997; Yun et al., 2013), ultimately these
72 all are again using different landmarks than FreeSurfer uses for cortical parcellations
73 (i.e., volume, thickness, surface area, gyrification). Note that, though FreeSurfer itself
74 does compute sulcal maps, these are computed as normalized depths, not in real-world
75 units (e.g. Kippenhan et al., 2005), furthermore, these are also independent of sulcal
76 width information.

77 Here I describe a procedure for estimating sulcal morphology and report
78 age-related differences in sulcal width and depth using three large samples of adults
79 across the lifespan: two of these datasets are from Western samples, Dallas Lifespan
80 Brain Study (DLBS) and Open Access Series of Imaging Studies (OASIS), as well as
81 well as one East Asian sample, Southwest University Adult Lifespan (SALD), as
82 potential differences between populations have been relatively understudied (Leong et
83 al., 2017; Madan, 2017). To further validate the method, test-retest reliability was also
84 assessed using a sample of young adults who were scanned ten times within the span
85 of a month (Chen et al., 2015; Madan & Kensinger, 2017b). All four of these datasets are
86 open-access and have sufficient sample sizes to be suitable for brain morphology
87 research (Madan, 2017). This procedure has been implemented as a MATLAB toolbox
88 that serves as an extension to FreeSurfer, `calcSulc`, that calculates sulcal
89 morphology—both width and depth—using files generated as part of the standard
90 FreeSurfer cortical reconstruction and parcellation pipeline. This toolbox is now made
91 freely available as supplemental to this paper:
92 <https://cmadan.github.io/calcSulc/>.

93 **2 Estimating sulcal morphology**

94 In this section I will outline the procedure and functionality of the `calcSulc` toolbox
95 that was designed to automate characterization of individual sulci, based on
96 intermediate files generated as part of the standard FreeSurfer analysis pipeline.

97 For each individual sulci (for each hemisphere and participant), the following
98 approach was used to characterize the sulcal morphology. First the pial surface and
99 Destrieux et al. (2010) parcellation labels were read into MATLAB by using the
100 FreeSurfer-MATLAB toolbox provided alongside FreeSurfer (`calcSulc_load`).
101 Using this, the faces associated with the individual sulci were isolated as a 3D mesh
102 (`calcSulc_isolate`).

103 The width of each sulci (`calcSulc_width`) was calculated by determining
104 which vertices lay on the boundary of the sulci and another region. An iterative
105 procedure was then used to determine the 'chain' of edges that would form a
106 contiguous edge-loop that encircle the sulci region (`calcSulc_getEdgeLoop`). This
107 provided an exhaustive list of all vertices that were mid-way between the peak of the
108 respective adjacent gyri and depth of the sulci itself. For each vertex in this edge-loop,
109 the nearest point in 3D space that was *not* neighbouring in the loop was determined,
110 with the goal of finding the nearest vertex in the edge that was on the opposite side of
111 the sulci—i.e., a line between these two vertices would 'bridge' across the sulcus. Since
112 these nearest vertices in the edge loop are not necessarily the nearest vertex along the
113 opposite sulcus wall, an exhaustive search (walk) was performed, moving up to a 4
114 edges from the initially determined nearest vertex (defined by
115 `options.setWidthWalk`). The sulci width was then taken as the median of these
116 distances that bridged across the sulci.

117 The depth of each sulci (`calcSulc_depth`) additionally used the FreeSurfer
118 sulcal maps (`?h.sulc`) to determine the relative inflections in the surface mesh, which
119 would be in alignment with the gyral crown. The deepest points of the sulcus, i.e., the
120 sulcal fundus, were taken as the 100 vertices within the sulcus with the lowest values
121 in the sulcal map. For these 100 vertices, the shortest distance to the smoothed
122 gyrification surface was calculated, and the median of these was then taken as the
123 sulcal depth.

124 Sulcal morphology, with and depth, was estimated for eight major sulci in each
125 hemisphere: central, post-central, superior frontal, inferior frontal, parieto-occipital,

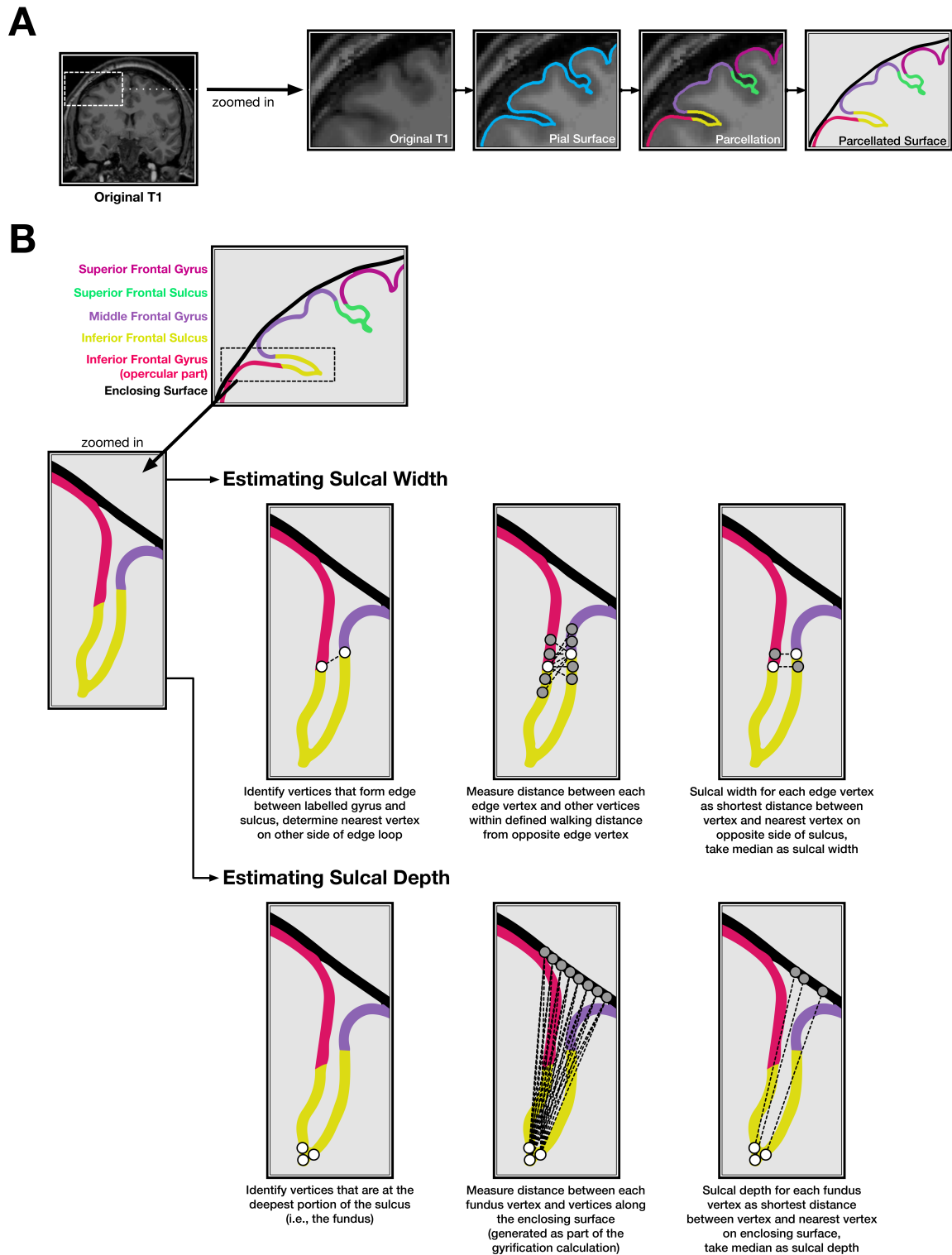


Figure 2. Illustration of the sulcal morphology method. (A) Cortical surface estimation and sulcal identification, as output from FreeSurfer. (B) Sulcal width and depth estimation procedure. Note that the surface mesh and estimation algorithm use many more vertices than shown here.

126 occipito-temporal, middle occipital and lunate, and marginal part of the cingulate (see
127 Figure 3). Sulcal boundaries were defined based on the Destrieux et al. (2010)
128 parcellation atlas (`S_central`, `S_postcentral`, `S_front_sup`, `S_front_inf`,
129 `S_parieto_occipital`, `S_oc-temp_med&Lingual`, `S_oc_middle&Lunatus`,
130 `S_cingul-Marginalis`).

131 3 Demonstration

132 3.1 Methods

133 3.1.1 Datasets

134 **3.1.1.1 OASIS.** This dataset consisted of 314 healthy adults (196 females), aged
135 18–94, from the Open Access Series of Imaging Studies (OASIS) cross-sectional dataset
136 (<http://www.oasis-brains.org>) (Marcus et al., 2007). Participants were
137 recruited from a database of individuals who had (a) previously participated in MRI
138 studies at Washington University, (b) were part of the Washington University
139 Community, or (c) were from the longitudinal pool of the Washington University
140 Alzheimer Disease Research Center. Participants were screened for neurological and
141 psychiatric issues; the Mini-Mental State Examination (MMSE) and Clinical Dementia
142 Rating (CDR) were administered to participants aged 60 and older. To only include

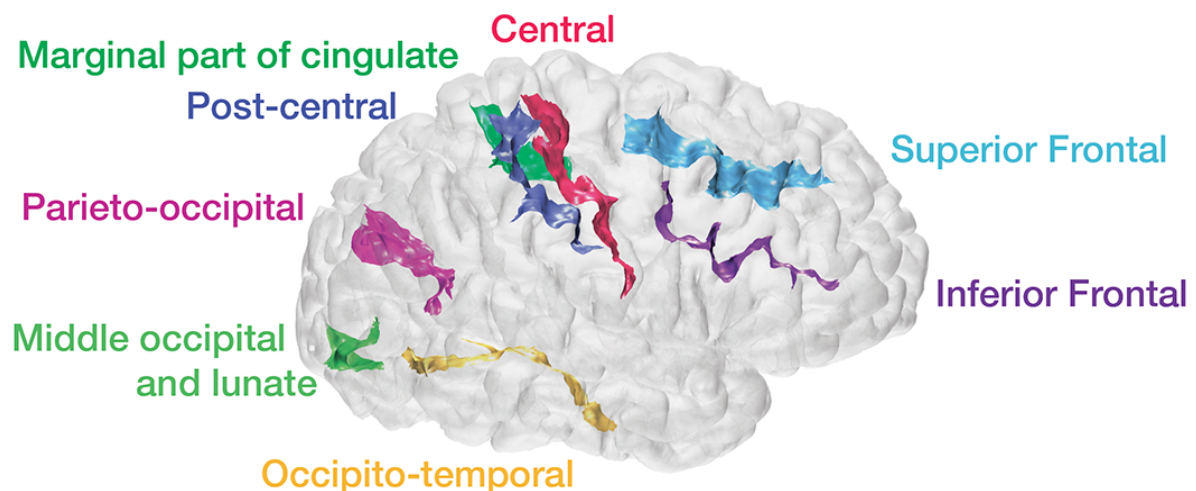


Figure 3. Example cortical surface with estimated sulci identified and labelled.

143 healthy adults, participants with a CDR above zero were excluded; all remaining
144 participants scored 25 or above on the MMSE. Multiple T1 volumes were acquired
145 using a Siemens Vision 1.5 T with a MPRAGE sequence; only the first volume was used
146 here. Scan parameters were: TR=9.7 ms; TE=4.0 ms; flip angle=10°;
147 voxel size=1.25×1×1 mm. Age-related comparisons for volumetric and fractal
148 dimensionality measures from the OASIS dataset were previously reported in Madan
149 and Kensinger (2017a), Madan and Kensinger (2018), and Madan (2018b) ¹.

150 **3.1.1.2 DLBS.** This dataset consisted of 315 healthy adults (198 females), aged
151 20–89, from wave 1 of the Dallas Lifespan Brain Study (DLBS), made available through
152 the International Neuroimaging Data-sharing Initiative (INDI) (Mennes et al., 2013)
153 and hosted on the Neuroimaging Informatics Tools and Resources Clearinghouse
154 (NITRC) (Kennedy et al., 2016)
155 (http://fcon_1000.projects.nitrc.org/indi/retro/dlbs.html).
156 Participants were screened for neurological and psychiatric issues. No participants in
157 this dataset were excluded *a priori*. All participants scored 26 or above on the MMSE.
158 T1 volumes were acquired using a Philips Achieva 3 T with a MPRAGE sequence. Scan
159 parameters were: TR=8.1 ms; TE=3.7 ms; flip angle=12°; voxel size=1×1×1 mm. See
160 Kennedy et al. (2015) and Chan et al. (2014) for further details about the dataset.
161 Age-related comparisons for volumetric and fractal dimensionality measures from the
162 DLBS dataset were previously reported in Madan and Kensinger (2017a), Madan and
163 Kensinger (2018), and Madan (2018b) ¹.

164 **3.1.1.3 SALD.** This dataset consisted of 483 healthy adults (303 females), aged
165 19–80, from the Southwest University Adult Lifespan Dataset (SALD) (Wei et al., 2018),
166 also made available through INDI and hosted on NITRC
167 (http://fcon_1000.projects.nitrc.org/indi/retro/sald.html). No
168 participants in this dataset were excluded *a priori*. T1 volumes were acquired using a

¹Note that analyses reported in these previous papers were based on preprocessing in FreeSurfer 5.3.0, rather than FreeSurfer 6.0.

169 Siemens Trio 3 T with a MPRAGE sequence. Scan parameters were: TR=1.9 s;
170 TE=2.52 ms; flip angle=9°; voxel size=1×1×1 mm.

171 **3.1.1.4 CCBD.** This dataset consisted of 30 healthy adults (15 females), aged 20–30,
172 from the Center for Cognition and Brain Disorders (CCBD) at Hangzhou Normal
173 University (Chen et al., 2015). Each participant was scanned for 10 sessions, occurring
174 2-3 days apart over a one-month period. No participants in this dataset were excluded
175 *a priori*. T1 volumes were acquired using a SCANNER with a FSPGR sequence. Scan
176 parameters were: TR=8.06 ms; TE=3.1 ms; flip angle=8°; voxel size: 1×1×1 mm. This
177 dataset is included as part of the Consortium for Reliability and Reproducibility
178 (CoRR) (Zuo et al., 2014) as HNU1. Test-retest comparisons for volumetric and fractal
179 dimensionality measures from the CCBD dataset were previously reported in Madan
180 and Kensinger (2017b)¹.

181 **3.1.2 Procedure**

182 **3.1.2.1 Preprocessing of MRI data** Data were analyzed using FreeSurfer 6.0
183 (<https://surfer.nmr.mgh.harvard.edu>) on a machine running Red Hat
184 Enterprise Linux (RHEL) 7.4. FreeSurfer was used to automatically volumetrically
185 segment and parcellate cortical and subcortical structures from the T1-weighted
186 images (Fischl, 2012; Fischl & Dale, 2000) FreeSurfer's standard pipeline was used (i.e.,
187 `recon-all`). No manual edits were made to the surface meshes, but surfaces were
188 visually inspected. Cortical thickness is calculated as the distance between the white
189 matter surface (white-gray interface) and pial surface (gray-CSF interface) .
190 Gyrfication was also calculated using FreeSurfer, as described in Schaer et al. (2012).
191 Cortical regions were parcellated based on the Destrieux et al. (2010) atlas, also part of
192 the standard FreeSurfer analysis pipeline.

193 **3.1.2.2 Estimating sulcal morphology** Using the method proposed here, sulcal
194 width and depth were estimated for eight major sulci in each hemisphere: central,
195 post-central, superior frontal, inferior frontal, parieto-occipital, occipito-temporal,

196 middle occipital and lunate, and marginal part of the cingulate (see Figure 3). Sulcal
197 boundaries were defined based on the Destrieux et al. (2010) parcellation atlas
198 (`S_central`, `S_postcentral`, `S_front_sup`, `S_front_inf`,
199 `S_parieto_occipital`, `S_oc-temp_med&Lingual`, `S_oc_middle&Lunatus`,
200 `S_cingul-Marginalis`).

201 Preliminary analyses additionally included superior and inferior temporal sulci
202 and intraparietal sulcus but these were removed from further analysis when the sulci
203 width estimation was found to fail to determine a closed boundary edge-loop at an
204 unacceptable rate ($> 10\%$) for at least one hemisphere. This edge boundary
205 determination failed when parcellated regions were labeled by FreeSurfer to comprise
206 at least two discontinuous regions, such that they could not be identified using a single
207 edge loop. Nonetheless, sulcal measures failed to be estimated for some participants,
208 resulting in final samples of 310 adults from the OASIS dataset, 312 adults from the
209 DLBS dataset, 481 adults from the SALD dataset, and 30 adults from the CCBD dataset.

210 **3.1.2.3 Test-retest reliability** Test-retest reliability was assessed as intraclass
211 correlation coefficient (*ICC*), which can be used to quantify the relationship between
212 multiple measurements (Asendorpf & Wallbott, 1979; Bartko, 1966; Chen et al., 2018;
213 Hallgren, 2012; Koo & Li, 2016; Madan & Kensinger, 2017b; Rajaratnam, 1960; Shrout &
214 Fleiss, 1979). McGraw and Wong (1996) provide a comprehensive review of the various
215 *ICC* formulas and their applicability to different research questions. *ICC* was
216 calculated as the one-way random effects model for the consistency of single
217 measurements, i.e., *ICC*(1, 1). As a general guideline, *ICC* values between .75 and
218 1.00 are considered 'excellent,' .60–.74 is 'good,' .40–.59 is 'fair,' and below .40 is 'poor'
219 (Cicchetti, 1994).

220 3.2 Results & Discussion

221 **3.2.0.1 Age-related differences in sulcal morphology** Scatter plots showing the
222 relationships between each individual sulci width and depth and age, for the OASIS

223 dataset, are shown in Figure 4; the corresponding correlations for all datasets are
224 shown in Tables 1 and 2. The width and depth of the central and post-central sulci
225 appear to be particularly correlated with age, with wider and shallower sulci in older
226 adults. Age-related differences in sulcal width and depth are generally present in
227 other sulci as well, but are generally weaker.

228 Age-related relationships for each sulci were relatively consistent between the
229 two Western lifespan datasets (OASIS and DLBS), but age-related differences in sulcal
230 width (but not depth) were markedly weaker in the East Asian lifespan dataset (SALD).
231 This finding will need to be studied further, but may be related to gross differences in
232 anatomical structure (Kochunov et al., 2003; Tang et al., 2010). Importantly, test-retest
233 reliability, $ICC(1, 1)$, was particularly good for the sulcal depth across individual sulci.

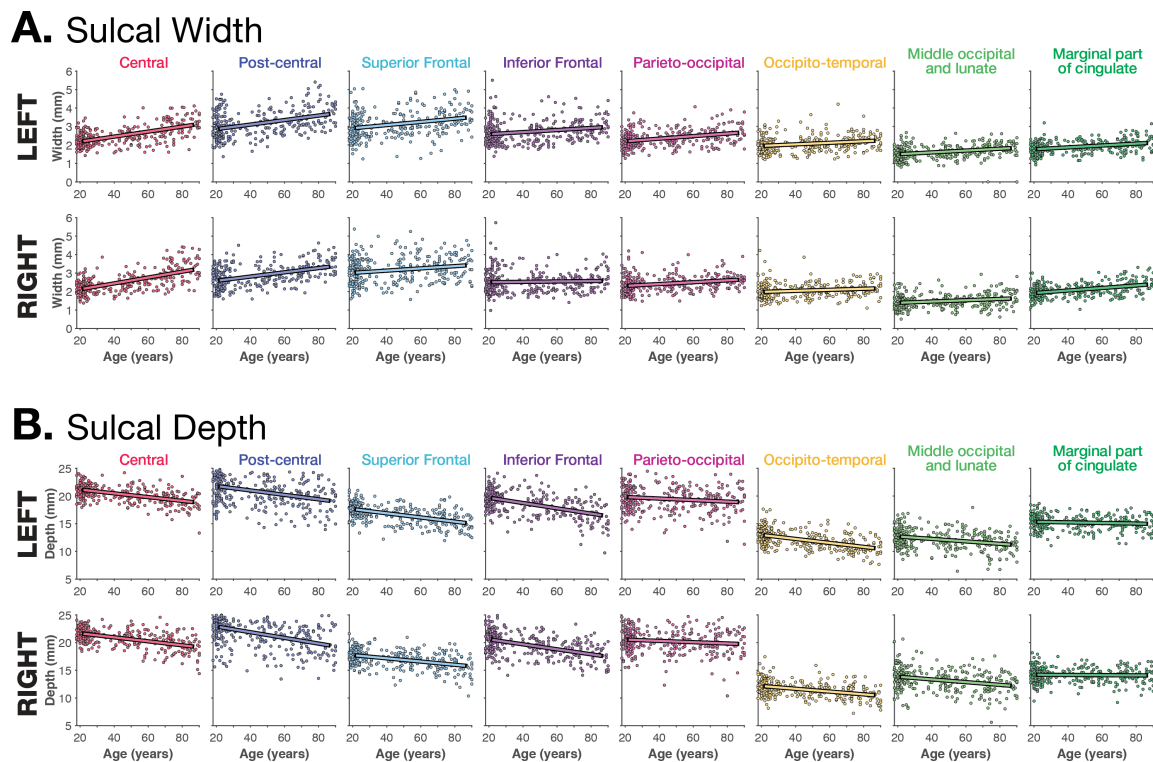


Figure 4. Relationship between (A) sulcal depth and (B) width for each of the sulci examined, based on the OASIS dataset.

234 To obtain a coarse summary measure across sulci, I averaged the sulcal width
235 across the 16 individual sulci for each individual, and with each dataset, and examined
236 the relationship between mean sulcal width with age. These correlations, shown in

SULCAL MORPHOLOGY

Sulci Name	FreeSurfer Label†	Hemi.	OASIS	DLBS	SALD	CCBD	
			<i>r</i> (Age)	<i>r</i> (Age)	<i>r</i> (Age)	<i>ICC</i> (1,1)	95% CI of <i>ICC</i>
Central	S_central	L	.586	.486	.322	.858	[0.785, 0.918]
		R	.632	.523	.294	.842	[0.764, 0.908]
Post-central	S_postcentral	L	.413	.391	.198	.764	[0.660, 0.858]
		R	.460	.436	.213	.864	[0.794, 0.922]
Superior Frontal	S_front_sup	L	.281	.421	.055	.797	[0.703, 0.880]
		R	.205	.291	.035	.843	[0.764, 0.909]
Inferior Frontal	S_front_inf	L	.217	.323	-.037	.775	[0.675, 0.865]
		R	.043	.222	-.036	.831	[0.748, 0.901]
Parieto-occipital	S_parieto_occipital	L	.348	.279	.145	.616	[0.486, 0.753]
Occipito-temporal	S_oc-temp_med&Lingual	R	.257	.357	.213	.682	[0.561, 0.802]
		L	.227	.270	-.055	.660	[0.535, 0.786]
Middle occipital and lunate	S_oc_middle&Lunatus	R	.168	.189	.017	.692	[0.572, 0.808]
		L	.306	.271	.145	.605	[0.474, 0.744]
Marginal part of cingulate	S_cingul-Marginalis	R	.212	.177	.023	.625	[0.496, 0.760]
		L	.340	.275	.075	.783	[0.685, 0.871]
		R	.430	.382	.161	.757	[0.651, 0.853]
<i>Mean</i>			.636	.592	.227	.907	[0.856, 0.947]

Table 1

Correlations between sulcal width and age for each sulci and hemisphere, for each of the three lifespan datasets examined. Test-retest reliability, ICC(1, 1), is also included from the CCBD dataset. †FreeSurfer labels in version 6.0; labels are named slightly different in version 5.3.

Sulci Name	FreeSurfer Label†	Hemi.	OASIS	DLBS	SALD	CCBD	
			<i>r</i> (Age)	<i>r</i> (Age)	<i>r</i> (Age)	<i>ICC</i> (1,1)	95% CI of <i>ICC</i>
Central	S_central	L	-.517	-.205	-.346	.848	[0.772, 0.912]
		R	-.505	-.256	-.348	.860	[0.789, 0.919]
Post-central	S_postcentral	L	-.371	-.264	-.268	.965	[0.944, 0.981]
		R	-.436	-.246	-.330	.890	[0.831, 0.937]
Superior Frontal	S_front_sup	L	-.523	-.454	-.397	.899	[0.844, 0.943]
		R	-.413	-.465	-.444	.886	[0.825, 0.935]
Inferior Frontal	S_front_inf	L	-.517	-.490	-.491	.932	[0.893, 0.962]
		R	-.496	-.480	-.490	.915	[0.868, 0.952]
Parieto-occipital	S_parieto_occipital	L	-.145	-.093	-.241	.979	[0.966, 0.989]
Occipito-temporal	S_oc-temp_med&Lingual	R	-.124	.059	-.229	.970	[0.952, 0.984]
		L	-.509	-.323	-.263	.953	[0.926, 0.974]
Middle occipital and lunate	S_oc_middle&Lunatus	R	-.404	-.316	-.281	.913	[0.864, 0.951]
		L	-.290	-.167	-.150	.949	[0.919, 0.972]
Marginal part of cingulate	S_cingul-Marginalis	R	-.288	-.120	-.132	.922	[0.879, 0.956]
		L	-.092	-.035	-.268	.952	[0.925, 0.974]
		R	-.032	-.017	-.156	.918	[0.872, 0.954]
<i>Mean</i>			-.465	-.645	-.600	.972	[0.955, 0.985]

Table 2

Correlations between sulcal depth and age for each sulci and hemisphere, for each of the three lifespan datasets examined. Test-retest reliability, ICC(1, 1), is also included from the CCBD dataset. †FreeSurfer labels in version 6.0; labels are named slightly different in version 5.3.

237 Table 1, indicate that the mean sulcal width was generally a better indicator of
238 age-related differences in sulcal morphology than individual sulci, and had increased
239 test-retest reliability. Mean sulcal depth was similarly more sensitive to age-related
240 differences than individual sulci (e.g., it is unclear why the relationship between age
241 and width of the central sulcus differed between samples) and the magnitude of this
242 relationship was more consistent across datasets. Reliability was even higher for mean
243 sulcal depth than mean sulcal width.

244 **3.2.0.2 Comparison with other age-related structural differences** Within each
245 dataset, mean sulcal depth and width correlated with age, as shown in Tables 1 and 2.
246 Of course, other measures of brain morphology also differ with age, such as mean
247 (global) cortical thickness [OASIS: $r(308) = -.793, p < .001$; DLBS: $r(310) = -.759,$
248 $p < .001$; SALD: $r(479) = -.642, p < .001$]. Additionally, volume of the third ventricle
249 (ICV-corrected) has been previously shown to significantly related to age (Madan &
250 Kensinger, 2017a; Walhovd et al., 2011), and was found to be true in each of the
251 examined lifespan datasets here as well [OASIS: $r(308) = .665, p < .001$; DLBS:
252 $r(310) = .677, p < .001$; SALD: $r(479) = .328, p < .001$].

253 To test if these mean sulcal measures served as distinct measures of age-related
254 differences in brain morphology, beyond those provided by other measures, such as
255 mean cortical thickness and volume of the third ventricle, I conducted partial
256 correlations that controlled for these two other measures of age-related atrophy. Mean
257 sulcal width [OASIS: $r_p(306) = .188, p < .001$; DLBS: $r_p(308) = .177, p = .002$; SALD:
258 $r(477) = .003, p = .96$] and depth [OASIS: $r_p(306) = -.443, p < .001$; DLBS:
259 $r_p(308) = -.397, p < .001$; SALD: $r_p(477) = -.534, p < .001$] both explained unique
260 variance in relation to age. Thus, even though more established measures of
261 age-related differences in brain morphology were replicated here, the additional sulcal
262 measures captured aspects of aging that are not accounted for by these extant
263 measures, indicating that these sulcal measures are worth pursuing further and are not
264 redundant with other measures of brain structure. Providing additional support for

265 this, mean sulcal width and depth were only weakly related to each other [OASIS:
266 $r(308) = -.192, p < .001$; DLBS: $r(310) = .092, p = .104$; SALD: $r(479) = .119, p = .009$].

267 As with the individual sulci measures, I did observe a difference between
268 samples where some age-related measures were less sensitive in the East Asian lifespan
269 sample (SALD), here in the ventricle volume correlation and the unsurprisingly
270 weaker age relationship in the partial correlation using sulcal width. These sample
271 differences are puzzling, though there is a general correspondence between the two
272 Western samples. Given that much of the literature is also based on Western samples, I
273 think further research with East Asian samples, and particularly comparing samples
274 with the same analysis pipeline, is necessary to shed further light on this initial finding.

275 **4 Conclusion**

276 Differences in sulcal width and depth are quite visually prominent, but are not often
277 quantified when examining individual differences in cortical structure. Here I
278 examined age-related differences in both sulcal measures as a proof-of-principle to
279 demonstrate the utility of the calcSulc toolbox that accompanies this paper and is
280 designed to closely compliment the standard FreeSurfer pipeline. This allows for the
281 additional measurement of sulcal morphology, to add to the extant measures of brain
282 morphology such as cortical thickness, area, and gyrification. Critically, this approach
283 uses the same landmarks and boundaries as in the Destrieux et al. (2010) parcellation
284 atlas, in contrast to all previous approaches to characterize sulcal features. This toolbox
285 is now made freely available as supplemental to this paper:

286 <https://cmadan.github.io/calcSulc/>.

287 Using this approach, here I demonstrate age-related differences in sulcal width
288 and depth, as well as high test-retest reliability. Since individual differences in sulcal
289 morphology are sufficiently distinct from those characterized by other brain
290 morphology measures, this approach should complement extant work of investigating
291 factors that influence brain morphology, e.g., see Figure 3 of Madan and Kensinger
292 (2018). Given the flexibility in the methodological approach, these measures can be

293 readily applied to other samples after being initially processed with FreeSurfer.

294 **Acknowledgments**

295 MRI data used in the preparation of this article were obtained from several sources,
296 data were provided in part by: (1) the Open Access Series of Imaging Studies (OASIS)
297 (Marcus et al., 2007); (2) wave 1 of the Dallas Lifespan Brain Study (DLBS) led by Dr.
298 Denise Park and distributed through INDI (Mennes et al., 2013) and NITRC (Kennedy
299 et al., 2016); (3) the Southwest University Adult Lifespan Dataset (SALD) (Wei et al.,
300 2018), also made available through INDI and hosted on NITRC; and (4) the Center for
301 Cognition and Brain Disorders (CCBD) (Chen et al., 2015) as dataset HNU1 in the
302 Consortium for Reliability and Reproducibility (CoRR) (Zuo et al., 2014).

References

303

304 Andersen, S. K., Jakobsen, C. E., Pedersen, C. H., Rasmussen, A. M., Plochanski, M., &
305 Østergaard, L. R. (2015). Classification of Alzheimer's disease from MRI using
306 sulcal morphology. In *Image analysis* (pp. 103–113). Springer International
307 Publishing. doi: 10.1007/978-3-319-19665-7_9

308 Andreasen, N. C., Harris, G., Cizadlo, T., Arndt, S., O'Leary, D. S., Swayze, V., & Flaum,
309 M. (1994). Techniques for measuring sulcal/gyral patterns in the brain as
310 visualized through magnetic resonance scanning: BRAINPLOT and BRAINMAP.
311 *Proceedings of the National Academy of Sciences*, 91, 93–97. doi: 10.1073/pnas.91.1.93

312

313 Asendorpf, J., & Wallbott, H. G. (1979). Maße der Beobachterübereinstimmung: ein
314 systematischer Vergleich. *Zeitschrift für Sozialpsychologie*, 10, 243–252.

315 Auzias, G., Brun, L., Deruelle, C., & Coulon, O. (2015). Deep sulcal landmarks:
316 Algorithmic and conceptual improvements in the definition and extraction of
317 sulcal pits. *NeuroImage*, 111, 12–25. doi: 10.1016/j.neuroimage.2015.02.008

318 Bartko, J. J. (1966). The intraclass correlation coefficient as a measure of reliability.
319 *Psychological Reports*, 19, 3–11. doi: 10.2466/pr0.1966.19.1.3

320 Beeston, C. J., & Taylor, C. J. (2000). Automatic landmarking of cortical sulci. In *Medical*
321 *image computing and computer-assisted intervention—MICCAI 2000* (pp. 125–133).
322 Springer Berlin Heidelberg. doi: 10.1007/978-3-540-40899-4_13

323 Behnke, K. J., Rettmann, M. E., Pham, D. L., Shen, D., Resnick, S. M., Davatzikos, C., &
324 Prince, J. L. (2003). Automatic classification of sulcal regions of the human brain
325 cortex using pattern recognition. In M. Sonka & J. M. Fitzpatrick (Eds.), *Medical*
326 *imaging 2003: Image processing*. SPIE. doi: 10.1117/12.480834

327 Cai, K., Xu, H., Guan, H., Zhu, W., Jiang, J., Cui, Y., ... Wen, W. (2017). Identification of
328 early-stage Alzheimer's disease using sulcal morphology and other common
329 neuroimaging indices. *PLOS ONE*, 12, e0170875. doi:
330 10.1371/journal.pone.0170875

331 Cao, B., Mwangi, B., Passos, I. C., Wu, M.-J., Keser, Z., Zunta-Soares, G. B., ... Soares,

- 332 J. C. (2017). Lifespan gyrification trajectories of human brain in healthy
333 individuals and patients with major psychiatric disorders. *Scientific Reports*, 7,
334 511. doi: 10.1038/s41598-017-00582-1
- 335 Chan, M. Y., Park, D. C., Savalia, N. K., Petersen, S. E., & Wig, G. S. (2014). Decreased
336 segregation of brain systems across the healthy adult lifespan. *Proceedings of the*
337 *National Academy of Sciences USA*, 111, E4997–E5006. doi:
338 10.1073/pnas.1415122111
- 339 Chen, B., Xu, T., Zhou, C., Wang, L., Yang, N., Wang, Z., ... Weng, X.-C. (2015).
340 Individual variability and test-retest reliability revealed by ten repeated
341 resting-state brain scans over one month. *PLOS ONE*, 10, e0144963. doi:
342 10.1371/journal.pone.0144963
- 343 Chen, G., Taylor, P. A., Haller, S. P., Kircanski, K., Stoddard, J., Pine, D. S., ... Cox, R. W.
344 (2018). Intraclass correlation: Improved modeling approaches and applications
345 for neuroimaging. *Human Brain Mapping*, 39, 1187–1206. doi: 10.1002/hbm.23909
346
- 347 Cicchetti, D. V. (1994). Guidelines, criteria, and rules of thumb for evaluating normed
348 and standardized assessment instruments in psychology. *Psychological Assessment*,
349 6, 284–290. doi: 10.1037/1040-3590.6.4.284
- 350 Coffey, C. E., Wilkinson, W. E., Parashos, L., Soady, S., Sullivan, R. J., Patterson, L. J., ...
351 Djang, W. T. (1992). Quantitative cerebral anatomy of the aging human brain: A
352 cross-sectional study using magnetic resonance imaging. *Neurology*, 42, 527–527.
353 doi: 10.1212/wnl.42.3.527
- 354 Destrieux, C., Fischl, B., Dale, A., & Halgren, E. (2010). Automatic parcellation of
355 human cortical gyri and sulci using standard anatomical nomenclature.
356 *NeuroImage*, 53, 1–15. doi: 10.1016/j.neuroimage.2010.06.010
- 357 Drayer, B. P. (1988). Imaging of the aging brain. Part I. normal findings. *Radiology*, 166,
358 785–796. doi: 10.1148/radiology.166.3.3277247
- 359 Elkis, H., Friedman, L., Wise, A., & Meltzer, H. Y. (1995). Meta-analyses of studies of
360 ventricular enlargement and cortical sulcal prominence in mood disorders.

- 361 *Archives of General Psychiatry*, 52, 735. doi: 10.1001/archpsyc.1995.03950210029008
- 362
- 363 Eskildsen, S. F., Uldahl, M., & Ostergaard, L. R. (2005). Extraction of the cerebral
364 cortical boundaries from MRI for measurement of cortical thickness. In
365 J. M. Fitzpatrick & J. M. Reinhardt (Eds.), *Medical imaging 2005: Image processing*.
366 SPIE. doi: 10.1117/12.595145
- 367 Fischl, B. (2012). FreeSurfer. *NeuroImage*, 62, 774–781. doi:
368 10.1016/j.neuroimage.2012.01.021
- 369 Fischl, B., & Dale, A. M. (2000). Measuring the thickness of the human cerebral cortex
370 from magnetic resonance images. *Proceedings of the National Academy of Sciences*
371 *USA*, 97, 11050–11055. doi: 10.1073/pnas.200033797
- 372 Fjell, A. M., Westlye, L. T., Amlie, I., Espeseth, T., Reinvang, I., Raz, N., ... Walhovd,
373 K. B. (2009). High consistency of regional cortical thinning in aging across
374 multiple samples. *Cerebral Cortex*, 19, 2001–2012. doi: 10.1093/cercor/bhn232
- 375 Hallgren, K. A. (2012). Computing inter-rater reliability for observational data: An
376 overview and tutorial. *Tutorials in Quantitative Methods for Psychology*, 8, 23–34.
377 doi: 10.20982/tqmp.08.1.p023
- 378 Hamelin, L., Bertoux, M., Bottlaender, M., Corne, H., Lagarde, J., Hahn, V., ... Sarazin,
379 M. (2015). Sulcal morphology as a new imaging marker for the diagnosis of early
380 onset Alzheimer's disease. *Neurobiology of Aging*, 36, 2932–2939. doi:
381 10.1016/j.neurobiolaging.2015.04.019
- 382 Hogstrom, L. J., Westlye, L. T., Walhovd, K. B., & Fjell, A. M. (2013). The structure of the
383 cerebral cortex across adult life: Age-related patterns of surface area, thickness,
384 and gyrification. *Cerebral Cortex*, 23, 2521–2530. doi: 10.1093/cercor/bhs231
- 385 Huckman, M. S., Fox, J., & Topel, J. (1975). The validity of criteria for the evaluation of
386 cerebral atrophy by computed tomography. *Radiology*, 116, 85–92. doi:
387 10.1148/116.1.85
- 388 Hutton, C., Draganski, B., Ashburner, J., & Weiskopf, N. (2009). A comparison between
389 voxel-based cortical thickness and voxel-based morphometry in normal aging.

- 390 *NeuroImage*, 48, 371–380. doi: 10.1016/j.neuroimage.2009.06.043
- 391 Im, K., Jo, H. J., Mangin, J.-F., Evans, A. C., Kim, S. I., & Lee, J.-M. (2010). Spatial
392 distribution of deep sulcal landmarks and hemispherical asymmetry on the
393 cortical surface. *Cerebral Cortex*, 20, 602–611. doi: 10.1093/cercor/bhp127
- 394 Jacoby, R. J., Levy, R., & Dawson, J. M. (1980). Computed tomography in the elderly: I.
395 The normal population. *British Journal of Psychiatry*, 136, 249–255. doi:
396 10.1192/bjp.136.3.249
- 397 John, J. P., Wang, L., Moffitt, A. J., Singh, H. K., Gado, M. H., & Csernansky, J. G. (2006).
398 Inter-rater reliability of manual segmentation of the superior, inferior and middle
399 frontal gyri. *Psychiatry Research: Neuroimaging*, 148, 151–163. doi:
400 10.1016/j.psychresns.2006.05.006
- 401 Jones, S. E., Buchbinder, B. R., & Aharon, I. (2000). Three-dimensional mapping of
402 cortical thickness using Laplace's equation. *Human Brain Mapping*, 11, 12–32. doi:
403 10.1002/1097-0193(200009)11:1<12::aid-hbm20>3.0.co;2-k
- 404 Kennedy, D. N., Haselgrove, C., Riehl, J., Preuss, N., & Buccigrossi, R. (2016). The
405 NITRC image repository. *NeuroImage*, 124, 1069–1073. doi:
406 10.1016/j.neuroimage.2015.05.074
- 407 Kennedy, K. M., Rodrigue, K. M., Bischof, G. N., Hebrank, A. C., Reuter-Lorenz, P. A.,
408 & Park, D. C. (2015). Age trajectories of functional activation under conditions of
409 low and high processing demands: An adult lifespan fMRI study of the aging
410 brain. *NeuroImage*, 104, 21–34. doi: 10.1016/j.neuroimage.2014.09.056
- 411 Kippenhan, J. S., Olsen, R. K., Mervis, C. B., Morris, C. A., Kohn, P., Meyer-Lindenberg,
412 A., & Berman, K. F. (2005). Genetic contributions to human gyrification: Sulcal
413 morphometry in Williams syndrome. *Journal of Neuroscience*, 25, 7840–7846. doi:
414 10.1523/jneurosci.1722-05.2005
- 415 Kochunov, P., Fox, P., Lancaster, J., Tan, L. H., Amunts, K., Zilles, K., ... Gao, J. H.
416 (2003). Localized morphological brain differences between english-speaking
417 caucasians and chinese-speaking asians: new evidence of anatomical plasticity.
418 *NeuroReport*, 14, 961–964. doi: 10.1097/01.wnr.0000075417.59944.00

- 419 Kochunov, P., Mangin, J.-F., Coyle, T., Lancaster, J., Thompson, P., Rivière, D., . . . Fox,
420 P. T. (2005). Age-related morphology trends of cortical sulci. *Human Brain*
421 *Mapping*, 26, 210–220. doi: 10.1002/hbm.20198
- 422 Kochunov, P., Rogers, W., Mangin, J.-F., & Lancaster, J. (2012). A library of cortical
423 morphology analysis tools to study development, aging and genetics of cerebral
424 cortex. *Neuroinformatics*, 10, 81–96. doi: 10.1007/s12021-011-9127-9
- 425 Kochunov, P., Thompson, P. M., Coyle, T. R., Lancaster, J. L., Kochunov, V., Royall, D.,
426 . . . Fox, P. T. (2008). Relationship among neuroimaging indices of cerebral health
427 during normal aging. *Human Brain Mapping*, 29, 36–45. doi: 10.1002/hbm.20369
- 428 Koo, T. K., & Li, M. Y. (2016). A guideline of selecting and reporting intraclass
429 correlation coefficients for reliability research. *Journal of Chiropractic Medicine*, 15,
430 155–163. doi: 10.1016/j.jcm.2016.02.012
- 431 Laffey, P. A., Peyster, R. G., Nathan, R., Haskin, M. E., & McGinley, J. A. (1984).
432 Computed tomography and aging: Results in a normal elderly population.
433 *Neuroradiology*, 26, 273–278. doi: 10.1007/BF00339770
- 434 Lamont, A. J., Mortby, M. E., Anstey, K. J., Sachdev, P. S., & Cherbuin, N. (2014). Using
435 sulcal and gyral measures of brain structure to investigate benefits of an active
436 lifestyle. *NeuroImage*, 91, 353–359. doi: 10.1016/j.neuroimage.2014.01.008
- 437 Largen, J. W., Smith, R. C., Calderon, M., Baumgartner, R., Lu, R. B., Schoolar, J. C., &
438 Ravichandran, G. K. (1984). Abnormalities of brain structure and density in
439 schizophrenia. *Biological Psychiatry*, 19, 991–1013.
- 440 Le Goualher, G., Barillot, C., Bizais, Y. J., & Scarabin, J.-M. (1996). Three-dimensional
441 segmentation of cortical sulci using active models. In M. H. Loew &
442 K. M. Hanson (Eds.), *Medical imaging 1996: Image processing*. SPIE. doi:
443 10.1117/12.237928
- 444 Le Goualher, G., Collins, D. L., Barillot, C., & Evans, A. C. (1998). Automatic
445 identificaion of cortical sulci using a 3d probabilistic atlas. In *Medical image*
446 *computing and computer-assisted intervention – MICCAI’98* (pp. 509–518). Springer
447 Berlin Heidelberg. doi: 10.1007/bfb0056236

- 448 Lee, J. K., Lee, J.-M., Kim, J. S., Kim, I. Y., Evans, A. C., & Kim, S. I. (2006). A novel
449 quantitative cross-validation of different cortical surface reconstruction
450 algorithms using MRI phantom. *NeuroImage*, *31*, 572–584. doi:
451 10.1016/j.neuroimage.2005.12.044
- 452 Lemaitre, H., Goldman, A. L., Sambataro, F., Verchinski, B. A., Meyer-Lindenberg, A.,
453 Weinberger, D. R., & Mattay, V. S. (2012). Normal age-related brain
454 morphometric changes: nonuniformity across cortical thickness, surface area and
455 gray matter volume? *Neurobiology of Aging*, *33*, 617.e1–617.e9. doi:
456 10.1016/j.neurobiolaging.2010.07.013
- 457 Leong, R. L., Lo, J. C., Sim, S. K., Zheng, H., Tandi, J., Zhou, J., & Chee, M. W. (2017).
458 Longitudinal brain structure and cognitive changes over 8 years in an east asian
459 cohort. *NeuroImage*, *147*, 852–860. doi: 10.1016/j.neuroimage.2016.10.016
- 460 Li, G., Liu, T., Nie, J., Guo, L., & Wong, S. T. C. (2008). A novel method for cortical
461 sulcal fundi extraction. In *Medical image computing and computer-assisted
462 intervention–MICCAI 2008* (pp. 270–278). Springer Berlin Heidelberg. doi:
463 10.1007/978-3-540-85988-8_33
- 464 Liu, T., Lipnicki, D. M., Zhu, W., Tao, D., Zhang, C., Cui, Y., ... Wen, W. (2012). Cortical
465 gyrification and sulcal spans in early stage Alzheimer's disease. *PLOS ONE*, *7*,
466 e31083. doi: 10.1371/journal.pone.0031083
- 467 Liu, T., Sachdev, P. S., Lipnicki, D. M., Jiang, J., Geng, G., Zhu, W., ... Wen, W. (2013).
468 Limited relationships between two-year changes in sulcal morphology and other
469 common neuroimaging indices in the elderly. *NeuroImage*, *83*, 12–17. doi:
470 10.1016/j.neuroimage.2013.06.058
- 471 Liu, T., Wen, W., Zhu, W., Kochan, N. A., Trollor, J. N., Reppermund, S., ... Sachdev,
472 P. S. (2011). The relationship between cortical sulcal variability and cognitive
473 performance in the elderly. *NeuroImage*, *56*, 865–873. doi:
474 10.1016/j.neuroimage.2011.03.015
- 475 Liu, T., Wen, W., Zhu, W., Trollor, J., Reppermund, S., Crawford, J., ... Sachdev, P.
476 (2010). The effects of age and sex on cortical sulci in the elderly. *NeuroImage*, *51*,

- 477 19–27. doi: 10.1016/j.neuroimage.2010.02.016
- 478 Lohmann, G., & von Cramon, D. Y. (2000). Automatic labelling of the human cortical
479 surface using sulcal basins. *Medical Image Analysis*, 4, 179–188. doi:
480 10.1016/s1361-8415(00)00024-4
- 481 Lohmann, G., von Cramon, D. Y., & Colchester, A. C. F. (2008). Deep sulcal landmarks
482 provide an organizing framework for human cortical folding. *Cerebral Cortex*, 18,
483 1415–1420. doi: 10.1093/cercor/bhm174
- 484 Madan, C. R. (2017). Advances in studying brain morphology: The benefits of
485 open-access data. *Frontiers in Human Neuroscience*, 11, 405. doi:
486 10.3389/fnhum.2017.00405
- 487 Madan, C. R. (2018a). Age differences in head motion and estimates of cortical
488 morphology. *PeerJ*, 6, e5176.
- 489 Madan, C. R. (2018b). Shape-related characteristics of age-related differences in
490 subcortical structures. *Aging & Mental Health*. doi:
491 10.1080/13607863.2017.1421613
- 492 Madan, C. R., & Kensinger, E. A. (2016). Cortical complexity as a measure of
493 age-related brain atrophy. *NeuroImage*, 134, 617–629. doi:
494 10.1016/j.neuroimage.2016.04.029
- 495 Madan, C. R., & Kensinger, E. A. (2017a). Age-related differences in the structural
496 complexity of subcortical and ventricular structures. *Neurobiology of Aging*, 50,
497 87–95. doi: 10.1016/j.neurobiolaging.2016.10.023
- 498 Madan, C. R., & Kensinger, E. A. (2017b). Test–retest reliability of brain morphology
499 estimates. *Brain Informatics*, 4, 107–121. doi: 10.1007/s40708-016-0060-4
- 500 Madan, C. R., & Kensinger, E. A. (2018). Predicting age from cortical structure across
501 the lifespan. *European Journal of Neuroscience*, 47, 399–416. doi: 10.1111/ejn.13835
- 502 Mangin, J.-F., Riviere, D., Cachia, A., Duchesnay, E., Cointepas, Y.,
503 Papadopoulos-Orfanos, D., ... Regis, J. (2004). Object-based morphometry of the
504 cerebral cortex. *IEEE Transactions on Medical Imaging*, 23, 968–982. doi:
505 10.1109/tmi.2004.831204

- 506 Mangin, J.-F., Rivière, D., Coulon, O., Poupon, C., Cachia, A., Cointepas, Y., ...
507 Papadopoulos-Orfanos, D. (2004). Coordinate-based versus structural
508 approaches to brain image analysis. *Artificial Intelligence in Medicine*, *30*, 177–197.
509 doi: 10.1016/s0933-3657(03)00064-2
- 510 Marcus, D. S., Wang, T. H., Parker, J., Csernansky, J. G., Morris, J. C., & Buckner, R. L.
511 (2007). Open Access Series of Imaging Studies (OASIS): Cross-sectional MRI data
512 in young, middle aged, nondemented, and demented older adults. *Journal of*
513 *Cognitive Neuroscience*, *19*, 1498–1507. doi: 10.1162/jocn.2007.19.9.1498
- 514 McGraw, K. O., & Wong, S. P. (1996). Forming inferences about some intraclass
515 correlation coefficients. *Psychological Methods*, *1*, 30–46. doi:
516 10.1037/1082-989x.1.1.30
- 517 McKay, D. R., Knowles, E. E. M., Winkler, A. A. M., Sprooten, E., Kochunov, P., Olvera,
518 R. L., ... Glahn, D. C. (2014). Influence of age, sex and genetic factors on the
519 human brain. *Brain Imaging and Behavior*, *8*, 143–152. doi:
520 10.1007/s11682-013-9277-5
- 521 Mennes, M., Biswal, B. B., Castellanos, F. X., & Milham, M. P. (2013). Making data
522 sharing work: The FCP/INDI experience. *NeuroImage*, *82*, 683–691. doi:
523 10.1016/j.neuroimage.2012.10.064
- 524 Mikhael, S., Hoogendoorn, C., Valdes-Hernandez, M., & Pernet, C. (2018). A critical
525 analysis of neuroanatomical software protocols reveals clinically relevant
526 differences in parcellation schemes. *NeuroImage*, *170*, 348–364. doi:
527 10.1016/j.neuroimage.2017.02.082
- 528 Ming, J., Harms, M. P., Morris, J. C., Beg, M. F., & Wang, L. (2015). Integrated cortical
529 structural marker for Alzheimer’s disease. *Neurobiology of Aging*, *36*, S53–S59. doi:
530 10.1016/j.neurobiolaging.2014.03.042
- 531 Nowinski, W. L., Raphel, J. K., & Nguyen, B. T. (1996). Atlas-based identification of
532 cortical sulci. In Y. Kim (Ed.), *Medical imaging 1996: Image display*. SPIE. doi:
533 10.1117/12.238488
- 534 Oguz, I., Cates, J., Fletcher, T., Whitaker, R., Cool, D., Aylward, S., & Styner, M. (2008).

- 535 Cortical correspondence using entropy-based particle systems and local features.
536 In *2008 5th IEEE International Symposium on Biomedical Imaging: From nano to*
537 *macro*. IEEE. doi: 10.1109/isbi.2008.4541327
- 538 Ono, M., Kubick, S., & Abernathy, C. D. (1990). *Atlas of the cerebral sulci*. Thieme.
539 Retrieved from
540 [https://www.amazon.com/Atlas-Cerebral-Sulci-Stefan-Kubik/](https://www.amazon.com/Atlas-Cerebral-Sulci-Stefan-Kubik/dp/3137321018?SubscriptionId=AKIAIOBINVZYXZQZ2U3A&tag=chimbori05-20&linkCode=xm2&camp=2025&creative=165953&creativeASIN=3137321018)
541 [dp/3137321018?SubscriptionId=AKIAIOBINVZYXZQZ2U3A&tag=](https://www.amazon.com/Atlas-Cerebral-Sulci-Stefan-Kubik/dp/3137321018?SubscriptionId=AKIAIOBINVZYXZQZ2U3A&tag=chimbori05-20&linkCode=xm2&camp=2025&creative=165953&creativeASIN=3137321018)
542 [chimbori05-20&linkCode=xm2&camp=2025&creative=](https://www.amazon.com/Atlas-Cerebral-Sulci-Stefan-Kubik/dp/3137321018?SubscriptionId=AKIAIOBINVZYXZQZ2U3A&tag=chimbori05-20&linkCode=xm2&camp=2025&creative=165953&creativeASIN=3137321018)
543 [165953&creativeASIN=3137321018](https://www.amazon.com/Atlas-Cerebral-Sulci-Stefan-Kubik/dp/3137321018?SubscriptionId=AKIAIOBINVZYXZQZ2U3A&tag=chimbori05-20&linkCode=xm2&camp=2025&creative=165953&creativeASIN=3137321018)
- 544 Palaniyappan, L., Park, B., Balain, V., Dangi, R., & Liddle, P. (2015). Abnormalities in
545 structural covariance of cortical gyrification in schizophrenia. *Brain Structure and*
546 *Function*, 220, 2059–2071. doi: 10.1007/s00429-014-0772-2
- 547 Pasquier, F., Leys, D., Weerts, J. G., Mounier-Vehier, F., Barkhof, F., & Scheltens, P.
548 (1996). Inter-and intraobserver reproducibility of cerebral atrophy assessment on
549 MRI scans with hemispheric infarcts. *European Neurology*, 36, 268–272. doi:
550 10.1159/000117270
- 551 Perrot, M., Rivière, D., & Mangin, J.-F. (2011). Cortical sulci recognition and spatial
552 normalization. *Medical Image Analysis*, 15, 529–550. doi:
553 10.1016/j.media.2011.02.008
- 554 Pizzagalli, F., Auzias, G., Kochunov, P., Faskowitz, J. I., Thompson, P. M., & Jahanshad,
555 N. (2017). The core genetic network underlying sulcal morphometry. In
556 E. Romero, N. Lepore, J. Brieva, & I. Larrabide (Eds.), *12th international symposium*
557 *on medical information processing and analysis*. SPIE. doi: 10.1117/12.2256959
- 558 Plochanski, M., & Østergaard, L. R. (2016). Extraction of sulcal medial surface and
559 classification of Alzheimer’s disease using sulcal features. *Computer Methods and*
560 *Programs in Biomedicine*, 133, 35–44. doi: 10.1016/j.cmpb.2016.05.009
- 561 Rajaratnam, N. (1960). Reliability formulas for independent decision data when
562 reliability data are matched. *Psychometrika*, 25, 261–271. doi: 10.1007/bf02289730
- 563 Reiner, P., Jouvent, E., Duchesnay, E., Cuingnet, R., Mangin, J.-F., & Chabriat, H. (2012).

- 564 Sulcal span in Alzheimer's disease, amnesic mild cognitive impairment, and
565 healthy controls. *Journal of Alzheimer's Disease*, 29, 605–613. doi:
566 10.3233/JAD-2012-111622
- 567 Rieder, R. O., Donnelly, E. F., Herdt, J. R., & Waldman, I. N. (1979). Sulcal prominence
568 in young chronic schizophrenic patients: CT scan findings associated with
569 impairment on neuropsychological tests. *Psychiatry Research*, 1, 1–8. doi:
570 10.1016/0165-1781(79)90021-0
- 571 Rivière, D., Mangin, J.-F., Papadopoulos-Orfanos, D., Martinez, J.-M., Frouin, V., &
572 Régis, J. (2002). Automatic recognition of cortical sulci of the human brain using
573 a congregation of neural networks. *Medical Image Analysis*, 6, 77–92. doi:
574 10.1016/s1361-8415(02)00052-x
- 575 Royackkers, N., Desvignes, M., Fawal, H., & Revenu, M. (1999). Detection and
576 statistical analysis of human cortical sulci. *NeuroImage*, 10, 625–641. doi:
577 10.1006/nimg.1999.0512
- 578 Salat, D. H., Buckner, R. L., Snyder, A. Z., Greve, D. N., Desikan, R. S. R., Busa, E., ...
579 Fischl, B. (2004). Thinning of the cerebral cortex in aging. *Cerebral Cortex*, 14,
580 721–730. doi: 10.1093/cercor/bhh032
- 581 Schaer, M., Cuadra, M. B., Schmansky, N., Fischl, B., Thiran, J.-P., & Eliez, S. (2012).
582 How to measure cortical folding from MR images: A step-by-step tutorial to
583 compute local gyrification index. *Journal of Visualized Experiments*, e3417. doi:
584 10.3791/3417
- 585 Scheltens, P., Pasquier, F., Weerts, J. G., Barkhof, F., & Leys, D. (1997). Qualitative
586 assessment of cerebral atrophy on MRI: Inter- and intra-observer reproducibility
587 in dementia and normal aging. *European Neurology*, 37, 95–99. doi:
588 10.1159/000117417
- 589 Shrout, P. E., & Fleiss, J. L. (1979). Intraclass correlations: Uses in assessing rater
590 reliability. *Psychological Bulletin*, 86, 420–428. doi: 10.1037/0033-2909.86.2.420
- 591 Sowell, E. R., Peterson, B. S., Kan, E., Woods, R. P., Yoshii, J., Bansal, R., ... Toga, A. W.
592 (2007). Sex differences in cortical thickness mapped in 176 healthy individuals

- 593 between 7 and 87 years of age. *Cerebral Cortex*, 17, 1550–1560. doi:
594 10.1093/cercor/bhl066
- 595 Sowell, E. R., Peterson, B. S., Thompson, P. M., Welcome, S. E., Henkenius, A. L., &
596 Toga, A. W. (2003). Mapping cortical change across the human life span. *Nature*
597 *Neuroscience*, 6, 309–315. doi: 10.1038/nn1008
- 598 Tang, Y., Hojatkashani, C., Dinov, I. D., Sun, B., Fan, L., Lin, X., ... Toga, A. W. (2010).
599 The construction of a chinese MRI brain atlas: A morphometric comparison study
600 between chinese and caucasian cohorts. *NeuroImage*, 51, 33–41. doi:
601 10.1016/j.neuroimage.2010.01.111
- 602 Thompson, P. M., Schwartz, C., Lin, R. T., Khan, A. A., & Toga, A. W. (1996).
603 Three-dimensional statistical analysis of sulcal variability in the human brain.
604 *Journal of Neuroscience*, 16, 4261–4274. doi: 10.1523/jneurosci.16-13-04261.1996
- 605 Tomlinson, B., Blessed, G., & Roth, M. (1968). Observations on the brains of
606 non-demented old people. *Journal of the Neurological Sciences*, 7, 331–356. doi:
607 10.1016/0022-510x(68)90154-8
- 608 Vaillant, M., & Davatzikos, C. (1997). Finding parametric representations of the cortical
609 sulci using an active contour model. *Medical Image Analysis*, 1, 295–315. doi:
610 10.1016/s1361-8415(97)85003-7
- 611 Walhovd, K. B., Westlye, L. T., Amlien, I., Espeseth, T., Reinvang, I., Raz, N., ... Fjell,
612 A. M. (2011). Consistent neuroanatomical age-related volume differences across
613 multiple samples. *Neurobiology of Aging*, 32, 916–932. doi:
614 10.1016/j.neurobiolaging.2009.05.013
- 615 Wei, D., Zhuang, K., Chen, Q., Yang, W., Liu, W., Wang, K., ... Qiu, J. (2018). Structural
616 and functional MRI from a cross-sectional Southwest University Adult Lifespan
617 Dataset (SALD). *bioRxiv*. doi: 10.1101/177279
- 618 Welker, W. (1990). Why does cerebral cortex fissure and fold? In E. G. Jones &
619 A. Peters (Eds.), *Cerebral cortex* (Vol. 8B, pp. 3–136). Springer US. doi:
620 10.1007/978-1-4615-3824-0_1
- 621 Yue, N. C., Arnold, A. M., Longstreth, W. T., Elster, A. D., Jungreis, C. A., O’Leary,

- 622 D. H., . . . Bryan, R. N. (1997). Sulcal, ventricular, and white matter changes at
623 MR imaging in the aging brain: Data from the cardiovascular health study.
624 *Radiology*, 202, 33–39. doi: 10.1148/radiology.202.1.8988189
- 625 Yun, H. J., Im, K., Yang, J.-J., Yoon, U., & Lee, J.-M. (2013). Automated sulcal depth
626 measurement on cortical surface reflecting geometrical properties of sulci. *PLOS*
627 *ONE*, 8, e55977. doi: 10.1371/journal.pone.0055977
- 628 Zuo, X.-N., Anderson, J. S., Bellec, P., Birn, R. M., Biswal, B. B., Blautzik, J., . . . Milham,
629 M. P. (2014). An open science resource for establishing reliability and
630 reproducibility in functional connectomics. *Scientific Data*, 1, 140049. doi:
631 10.1038/sdata.2014.49